# Parametrization of exact-finite-range distorted-wave Born approximation overlap integral for reactions induced by heavy ions

T. Udagawa, T. Tamura, and D. Price

*Department of Physics, University of Texas, Austin, Texas 78712*

(Received 21 September 1979)

In a few recent publications, which utilized exact-finite-range distorted-wave Born approximation, we successfully fitted continuum spectra observed in a variety of heavy-ion reactions. In making it feasible to carry out the numerical calculations involved, we found the use of properly parametrized transition amplitudes was very powerful and almost indispensable. In the present article, methods used for this parametrization are explained in detail.

## I. INTRODUCTION

The direct reaction (DR) theories have been used very successfully and extensively in recent years, in order to analyze data of reactions leading to discrete nuclear states. More recently attempts have been made to extend these theories to analyze data of reactions leading to the continuum. This extension was first carried out successfully for the analyses of light-ion induced reactions,[1] and then later for heavy-ion induced reactions.[2-5] There are two sets of key quantities that are to be calculated in applying DR theory to continuum data, the DR cross sections and the spectroscopic densities.[1] When light-ion induced continuum reactions are studied, the DR cross sections can be evaluated in very much the same way as they are for discrete state transitions. To do the same for heavy-ion induced reactions is, however, often too involved and practically impossible. The obvious reason for this is that for heavy-ion processes we have to use the exact-finite-range distorted-wave Born approximation (EFR-DWBA) and also have to consider a huge number of partial waves and transferred angular momenta.

Fortunately, however, for heavy-ion reactions, the transition amplitudes, or equivalently the overlap integrals of the DWBA theory, admit a very simple parametrization,[6,7] even when an EFR approach is used. They are rather accurately expressed in terms of a very simple analytic function, which involves only a few parameters, as well as quantum numbers. One thus needs to perform accurate evaluation of the overlap integrals only for selected sets of quantum numbers and energies, and the results are used to fix the parameters in the assumed analytic function. Once this parametrization is done, the DR cross section can be generated rather quickly.

The first successful application[2] of this parametrization technique was made to the analysis of the $(^{20}\text{Ne}, ^{16}\text{O})$ and $(^{20}\text{Ne}, ^{12}\text{C})$ reactions on an $^{27}\text{Al}$ target with $E_{\text{lab}}(^{20}\text{Ne}) = 120$ MeV.[8] It was assumed that the $(^{20}\text{Ne}, ^{16}\text{O})$ reaction proceeded as a one-step transfer of an alpha particle, while the $(^{20}\text{Ne}, ^{12}\text{C})$ reaction was a successive transfer of two alpha particles. It was found that we were able to fit rather nicely, not only the spectral shapes, but also the relative magnitudes of the $^{16}\text{O}$ and $^{12}\text{C}$ cross sections.

The same technique was then found[3] to be extremely powerful in explaining the spectrum and the polarization of $^{12}\text{B}$ observed in the $^{100}\text{Mo}$ $(^{14}\text{N}, ^{12}\text{B})$ $^{102}\text{Ru}$ reaction.[9] As explained in some detail in Ref. 3, we went one step further there in carrying out the calculations analytically. Thus after the overlap integrals were expressed analytically, several geometrical factors involved in the transition amplitude were also expressed analytically, by using their asymptotic forms. This made it possible to perform the summations over quantum numbers analytically also, bringing the transition amplitude into a closed analytic form. We were then able to obtain a good physical insight into what was taking place in the reaction, in particular demonstrating very clearly the crucial role played by the so-called recoil effect.

The work of Refs. 2 and 3 was further extended more recently to somewhat more complicated processes,[4,5] again very successfully. We have thus been convinced that the method we have developed indeed has a wide applicability. In our previous publications,[2-5] however, not much detail has been presented of how the parametrization procedure was carried out. To discuss this useful approach in detail is the purpose of the present article.

For the sake of clarity of presentation, we shall restrict ourselves in the present paper, for the

most part, to the ($^{14}$N, $^{12}$B) reaction of Ref. 9, which was studied in Ref. 3. In Sec. II, we first present the analytic form for the overlap integrals, which is a product of four factors. We then explain, step by step, how each of these factors emerged and how the parameters involved were fixed. Two of the four factors have Gaussian forms, representing the rather well known $l$-window effects. Another factor, called $N_0$, had not been investigated in the past, however, and we found that its behavior was fairly complicated.

We thus take up this $N_0$ factor anew in Sec. III, and investigate the origin of its peculiar behavior. The answer we have found is that $N_0$ copies rather faithfully the behavior of the form factors. In other words, what we found is that, once the behavior of the form factor is known, which is a comparatively easy thing to achieve, one can predict the behavior of the $N_0$ factor. Since the fourth factor in the analytic expression of the overlap integral is nothing but a phase factor coming from the two distorted waves involved, we thus have a complete knowledge of what functional form should be adopted to parametrizing the overlap integrals.

A few final remarks will be presented in Sec. IV.

## II. PARAMETRIZATION OF THE DWBA OVERLAP INTEGRALS

The DWBA overlap integrals which we are to evaluate may be written using the notation, e.g., of Ref. 12, as

$$I_{l_b l l_a}^{l_1 l_2}(E_b, E_a) = (k_a k_b)^{-1}$$
$$\times \int \chi_{l_b}(r_b) F_{l_b l l_a}^{l_1 l_2}(r_b, r_a) \chi_{l_a}(r_a) dr_a dr_b .$$

$$(1)$$

Here $\chi_{l_a}$ and $\chi_{l_b}$ are the distorted waves in the incident and exit channels, respectively, while $F_{l_b l l_a}^{l_1 l_2}(r_b, r_a)$ is the EFR form factor.

The above overlap integrals depend, among other things, on the orbital angular momenta $l_a$ and $l_b$ of the partial waves. They also depend on the channel energies $E_a$ and $E_b$, but we are normally concerned with a fixed incident energy $E_a$, thus making (1) depend more directly on the reaction $Q$ value, $Q = E_b - E_a$.

The overlap integrals further depend on $l_1$ and $l_2$, the orbital angular momenta which, in the specific example of the $^{100}$Mo($^{14}$N, $^{12}$B)$^{102}$Ru reaction, the center of mass of the two transferred protons has, respectively, in $^{102}$Ru and $^{14}$N, relative to the cores $^{100}$Mo and $^{12}$B. It was shown in Ref. 3 that we can treat the above process by assuming that the two protons are coupled to an internal spin equal to zero, and that we can fix $l_2$

$= 2$. As for $l_1$, let the spin of a final state of $^{102}$Ru be denoted by $I_B$. Since the internal spin of the two protons vanishes, and the target $^{100}$Mo has $I_A = 0$, we have $l_1 = I_B$. The transferred orbital angular momentum $l_1$ which must satisfy the triangular condition $\vec{l} = \vec{l}_1 + \vec{l}_2$, then takes five values for fixed $l_1$: $l = l_1 \pm 2$, $l_1 \pm 1$, and $l_1$. Among them, $l = l_1 \pm 2$ and $l_1$ are of normal parity since $l + l_1 + l_2$ = even, while $l = l_1 \pm 1$ are of non-normal parity since $l + l_1 + l_2 =$ odd.

It is important to remark here that the radial part of the wave function, describing the motion of the center of mass of transferred nucleons in the recipient nucleus, and consequently the form factors, may in general depend on the reaction $Q$ value, as well as on $l_1$. Normally, however, we ignore this $Q$ dependence, and construct the above radial wave function once and for all corresponding to a $Q$ value appropriate for the ground-state to ground-state transition. [See Ref. 1 for an argument justifying this treatment.] To remove this assumption of the $Q$ independence, however, does not make our procedure tremendously more complicated than it is with this assumption. It is true that we then have to reconstruct the form factor at each $Q$. However, as seen below, we actually construct the overlap integral (1) for a very restricted number of $Q$ values anyway, even when a $Q$-independent form factor is used.

We now claim that the above overlap integral can be represented, to a good approximation, by an analytic function of the form

$$I_{l_b l l_a}(E_b, E_a) = N_0(l_1 l_2 l l_a l_b) \exp[-(l_b - l_b^{(0)})^2 / \Gamma_b^2]$$
$$\times \exp[-(l_d - l_d^{(0)})^2 / \Gamma_d^2] \exp(i\delta), \quad (2a)$$

with

$$l_d = l_b - l_a , \quad (2b)$$

$$\Gamma_i = \alpha_i + \beta_i Q \quad (i = b \text{ or } d), \quad (2c)$$

$$l_i^{(0)} = \gamma_i + \epsilon_i Q \quad (i = b \text{ or } d), \quad (2d)$$

$$\delta = \delta_{l_a} + \delta_{l_b} \simeq \psi_0 + (l_b - l_b^{(0)})\psi_1(Q) . \quad (2e)$$

The quantity $\delta_{l_a}$ in (2e) is the real part of the phase shift of the elastic scattering in the incident channel, and similarity $\delta_{l_b}$ is that for the exit channel.

A feature to be noted in (2a) is that $I$ is characterized by two $l$ localizations, introducing two windows in the $l$ space. We refer to them as $l_b$ and $l_d$ windows henceforth. The origin of these windows has been discussed in the literature; see e.g., Ref. 7. In short, it is the peripheral nature of the direct reactions which enforces a good kinematic matching, in order for the cross sections to have significant values. The centers $l_i^{(0)}$ and the widths $\Gamma_i$ ($i = b$ or $d$) of these windows generally depend on $Q$, and as seen in (2c) and (2d), we

have assumed linear forms. The validity of this choice will soon be demonstrated.

The right-hand side of (2a) includes in it another real factor $N_0$, and we shall later discuss in detail its dependence on various angular momenta. The last factor of (2a) has a unit magnitude and is the only complex factor in (2a). The choice of $\delta$ as a sum of two phase shifts, as given in the first equality of (2e), is very reasonable because of the following facts.

As seen in (1), the origin of the complex nature of $I$ is the two distorted waves in the integrand. Since the heavy ions are strongly absorptive, each distorted wave consists (in the peripheral region) predominantly of the outgoing wave, whose phase is given closely by the real part of the phase shift of the elastic scattering. The phase factors which the two distorted waves thus acquire are then maintained as they are, even after the integration in (1) is carried out, making it imperative for $I$ to have the phase factor it is seen to have in (2a). That the phase $\delta$ can be expanded linearly in $l_b$, introducing in the course of expansion the deflection angle $\psi_1$, as seen by the second equality of (2e), is rather well known,[7] and we shall not discuss this feature further here.

Once the phase factor of (2a) has been understood in this way, we may concentrate our interest and discussion on the magnitude of $I$, i.e., on how the functional forms of the first three factors of (2a) were chosen and how the parameters involved were fixed. This process of parametrization must of course be preceded by that of the EFR-DWBA evaluation of $I$, for a large but nevertheless limited number of sets of values of $Q$, $l_a$, $l_b$ and $l$. [In the example of the ($^{14}$N, $^{12}$B) reaction,[3] this number was about 3000.] Somewhat crudely, it is proportional to the number of different $l$'s (for a fixed $l_1$), i.e., to $(2l_2 \pm 1)$. Therefore, it can be much smaller if, e.g., $l_2 = 0$. Once a sufficient number of the $|I|$ values, which we shall henceforth call "data," are accumulated, their parametrization proceeds as follows.

The first step is to fit the magnitude of the data, i.e., $|I|$. as close as possible by a function of the form

$$|I| = N_1 \exp[-(l_b - l_b^{(0)})^2/\Gamma_b^2] . \tag{3}$$

Clearly this function has $l_b$ as its only independent variable. In this fitting procedure, the values of the parameters $l_b^{(0)}$, $\Gamma_b$, and $N_1$ are obtained as functions of $Q$, as well as of the quantum numbers $l_a$, $l_1$, and $l$. It was found, however, that, although $l_b^{(0)}$ and $\Gamma_b$ did depend on $Q$, their dependence on $l_a$, $l_1$, and $l$ was rather weak. We thus decided to ignore the latter dependence entirely.

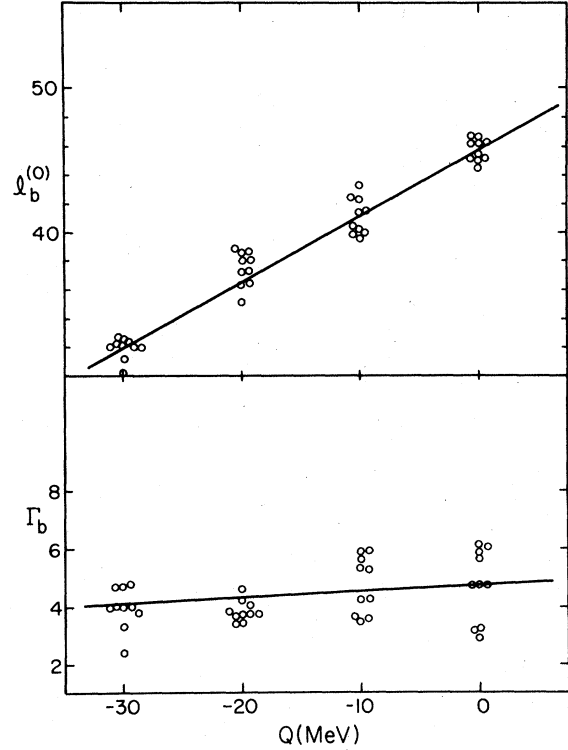In order to show the situation more explicitly,



FIG. 1. $\chi^2$-fit determined values of $l_b^{(0)}$ and $\Gamma_b$, based on (3). Circles represent as example the values calculated for $(l_1, l) = (10, 10)$ and $(10, 12)$ with $l_a = -4(-2)-12$. To be precise, all circles should appear on vertical lines corresponding to appropriate $Q$ values, horizontal displacement being employed simply to avoid overlapping. As discussed in the text $\chi^2$-fitting yields $l_b^{(0)} = 50.2 + 0.458Q$ and $\Gamma_b = 4.9 + 0.2Q$.

we plot in Fig. 1 the $\chi^2$-fitted values of $l_b^{(0)}$ and $\Gamma_b$, calculated for four choices of the $Q$ values. In this figure, these values of $l_b^{(0)}$ and $\Gamma_b$ are represented by open circles, each circle corresponding to a given set of $l_a$, $l_1$, and $l$. It is seen that these circles are nicely clustered together for each $Q$, showing the fairly weak dependence on the three quantum numbers.

Figure 1 further shows that the centers of the clusters of the circles lie very nicely on straight lines, justifying the choice of the linear dependence of $l_b^{(0)}$ and $\Gamma_b$ on $Q$ in Eqs. (2c) and (2d). The straight lines drawn in Fig. 1 have coefficients $\alpha_b$, $\beta_b$, $\gamma_b$, and $\epsilon_b$ determined so that these lines represent best, in the sense of $\chi^2$, the centers of the clusters of the circles, as functions of $Q$.

The second step of the parametrization begins by first expressing the coefficient $N_1$, whose values have been derived in the above first step of fitting, as

$$N_1 = N_0 \exp[-(Q - Q_0)^2/\Gamma_Q^2] . \tag{4}$$

The reader may wonder why a Gaussian function of $Q$, rather than of $l_d$, as was the case in (2a), is introduced here. The reason is that $|l_d|$ cannot exceed a given value of $l$, making it impossible to obtain enough sampling of the $N_1$ for a sufficiently wide range of the values of $l_d$. With the form of (4), this difficulty can be avoided.

By using (4), the values of $N_0$, $Q_0$, and $\Gamma_Q$ can be fixed as functions of $l_d$, $l_1$, and $l$. It was first found that $Q_0$ in practice depended only on $l_d$, and that this dependence was linear:

$$Q_0 = q_0 + q_1 l_d , \qquad (5)$$

the coefficients $q_0$ and $q_1$ being fixed again by a $\chi^2$ fit. It was further found that $\Gamma_Q$ could be taken simply as a constant. Therefore, Eq. (4) can now be replaced by

$$N_1 = N_0 \exp[-(l_d - l_d^{(0)})^2 / \Gamma_d^2] , \qquad (6)$$

recovering the coveted Gaussian factor that depends on $l_d$. Obviously the following relations hold, to express the parameters in (2) in terms of $\Gamma_Q$, $q_0$ and $q_1$:

$$l_d^{(0)} = -(q_0/q_1) + Q/q_1 , \quad \Gamma_d = \Gamma_Q/q_1 ,$$

$$\alpha_d = \Gamma_Q/q_1 , \quad \beta_d = 0 , \quad \gamma_d = -q_0/q_1$$

and

$$\epsilon_d = 1/q_1 . \qquad (7)$$

In order to show how good this parametrization really is, we have plotted in Fig. 2(a) the values of $N_1$ [actually of $-\ln(N_1)$] obtained in the above first step of parametrization, for four chosen sets of $l_d$ and $l_1$ values, and four different $Q$ values. They are to be compared with the solid lines representing the $N_1$ values obtained from the use of Eq. (6), and the agreement is seen to be good. In Fig. 2(b), on the other hand, comparison is made between the values of calculated $l_d$, as a function of $Q_0$, and the $l_d$ expressed in terms of (5). They agree very nicely with one another, justifying the linear dependence chosen in (5).

The second procedure for parametrization also yields the values of $N_0$, obtained as a function of $Q$, $l_d$, $l_1$, and $l$. A nice feature found was that $N_0$ was in practice independent of $Q$, indicating that the $Q$ dependence of $|I|$, i.e., the dependence of $|I|$ on the reaction dynamics, has been well incorporated into the two Gaussian factors that were derived above.

In order to illustrate the dependence of $N_0$ on the angular momentum quantum numbers, we show in Fig. 3(a) its values plotted as functions of $l_d$, for all the possible five values of $l$ ($=l_1 - 2 \sim l_1 + 2$) and for two choices of $l_1$, $l_1 = 6$ and 10.

A number of interesting features are seen in this figure. First of all, we observe that two curves with different $l_1$ but the same $\Delta(=l - l_1)$ behave
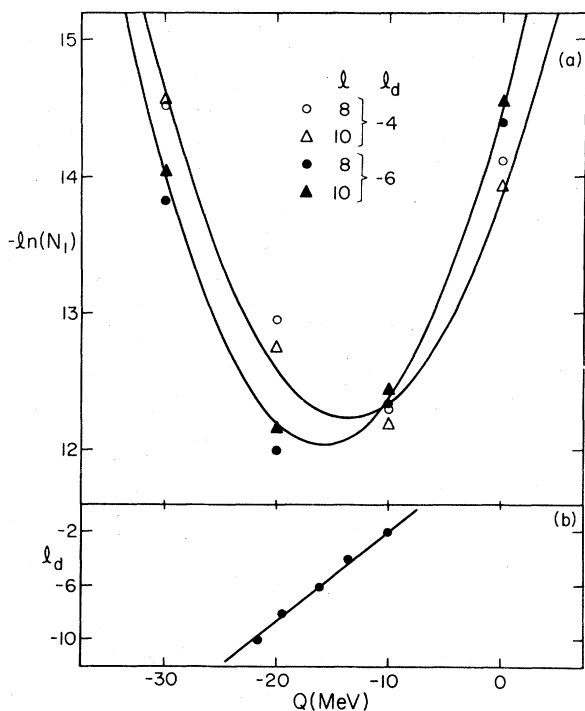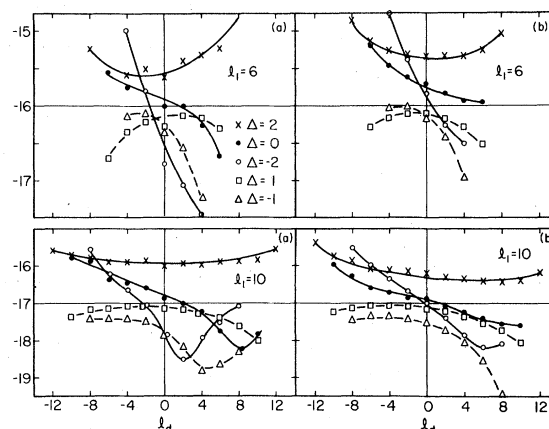


FIG. 2. (a) $\chi^2$-fit values of $-\ln(N_1)$ determined for $(l_1, l) = (10,8)$ and $(10,10)$, and for $l_d = -4$ and $-6$. Curves drawn are represented by $-\ln(N_1) = 0.01 \, (Q - Q_0)^2 + C$ with $Q_0 = -13.6$ and $-15.9$ (MeV) and $C = 12.24$ and 12.04, respectively, for $l_d = -4$ and $-6$: (b) $l_d$ as function of $Q_0$. Straight line represents $\chi^2$ fit as given by $l_d = 0.667 Q_0 + 4.67$.



FIG. 3. (a) $\ln(N_0) - 4.4$ as determined by $\chi^2$-fit. (b) $\ln(F)$ plotted as function of $l_d$. In (a), a subtraction of 4.4 has been made in order to facilitate the comparison of the two sets of quantities. In (b), the values of $F$ as determined by (9) have not been altered. The curves were drawn simply as guides.

TABLE I. Parameters that appear in Eq. (8).

| $\Delta$ | $\kappa_1$ | $\kappa_2$ | $\kappa_3 \times 10^2$ | $\kappa_4 \times 10^2$ | $\kappa_5 \times 10^2$ | $\kappa_6 \times 10^2$ |
|---|---|---|---|---|---|---|
| 2 | $-13.9$ | $-0.225$ | 4.69 | $-0.80$ | 0.90 | $-0.059$ |
| 1 | $-14.6$ | $-0.250$ | $-0.25$ | $-0.38$ | $-1.26$ | 0.071 |
| 0 | $-14.7$ | $-0.225$ | $-1.50$ | $-1.00$ | 0.0 | 0.0 |
| $-1$ | $-14.3$ | $-0.325$ | $-9.38$ | $-0.31$ | $-4.61$ | 0.353 |
| $-2$ | $-15.2$ | $-0.075$ | $-7.30$ | 0.40 | 0.0 | 0.0 |

very similarly. The curves with $\Delta = 2$ depend on $l_4$ weakly but quadratically. Those with $\Delta = 0$ and $-2$ are approximately linear in $l_4$, the latter having a gradient steeper than the former. All these three curves with even $\Delta$, i.e., those with normal parity, share a common feature in that they increase as $|l_4|$ increases with $l_4 < 0$. Compared with them, those with odd $\Delta(= \pm 1)$ decrease with increasing $|l_4|$, the dependence being approximately quadratic.

Similar features were seen for other values of $l_1$ also, and combining these results, we found that the following expression gives a good description of the angular momentum dependence of $N_0$:

$$N_0 = \exp[\kappa_1 + \kappa_2 l_1 + (\kappa_3 + \kappa_4 l_1)l_4 + (\kappa_5 + \kappa_6 l_1)l_4^2] . \qquad (8)$$

The parameters $\kappa_1 \sim \kappa_6$ are dependent on $\Delta$. Their values are summarized in Table I.

Equation (8) with the parameter values of Table I was actually used in the calculation made in Ref. 3. As seen, the angular momentum dependence of $N_0$ is somewhat complicated. This has, however, to a large extent been brought about because we have chosen as an example the reaction $(^{14}N, ^{12}B)$ for which $l_2 = 2$, allowing $\Delta$ to take five different values. In the case, e.g., of an $\alpha$-transfer reaction leading a $0^+$ projectile to a $0^+$ ejectile, we have $l_2 = 0$. This then allows a single $\Delta$ $(=0)$, making $N_0$ be given by (8) with a single set of $\kappa_1 \sim \kappa_6$ parameters. Then the factor $N_0$ is not much more complicated than are the other factors of (2a). In practice the use of (8) is not so tedious, however, even when several $\Delta$'s are permissible.

### III. ORIGIN OF THE ANGULAR MOMENTUM DEPENDENCE OF $N_0$

The physical origin of the $l$ window is well known,[7] and thus the appearance of the two Gaus-

sian factors in (2a) was not unexpected. The rather complicated dependence of the factor $N_0$ on angular momenta, as found towards the end of the last section, was on the other hand somewhat unexpected. Unless the origin of this peculiar behavior of $N_0$ is found, our task of fully understanding the behavior of the DWBA overlap integrals remains incomplete, and the significance of the parametrization we have achieved might remain suspect. We thus attempted to find the physical origin of Eq. (8), and it appears that we have succeeded. Because of this, we now feel that the choice of the functional form of (8) has a good physical justification, and a rather universal validity.

The key step which helped to find the origin we sought for was to recognize a surprisingly close similarity between the behaviors of $N_0$ and of the form factors. This can be seen, e.g., by comparing the curves in Fig. 3(a) with those in Fig. 3(b), which represent peak values (in the peripheral region) of the form factors associated with various sets of three angular momenta. The choice of these sets was made in the same way as in Fig. 3(a), and the similarity of the corresponding curves in these two figures is evident. (To be more precise, the stated similarity gets somewhat poorer for large positive $l_4$'s. For practical purposes, however, this causes no serious problem, because as we emphasized, particularly in Ref. 3, it is the large negative $l_4$'s that contribute dominantly to most continuum spectra.)

Once the above similarity is found, it is clear that the behavior of $N_0$ is understood, if that of the form factor is understood. In the rest of this section, we shall thus concentrate on the latter.

For this purpose, we find it very convenient to use the following expression for the EFR form factor, which was derived in our recent reformulation[10]:

$$F^{l_1 l_2}_{l_b l l_a}(r_b, r_a) = \tfrac{1}{2}[(4\pi)^{3/2}/(2l+1)] \hat{l}_b i^{l_a + l_b + l_1 + l_2}$$

$$\times \sum_{m_1 m m_2} (l_a m_1 l_b 0 | l m_1)(l_1 m_1 l_2 m_2 | l - m_1)(-)^{l + m_1}[2/(1 + \delta_{m_1,0})] \int W_{l_1}(r_1) W_{l_2}(r_2) Y_{l_a m_1}(\theta) Y_{l_1 m_1}(\theta_1)$$

$$\times Y_{l_2 m_2}(\theta_2) d\mu . \qquad (9)$$

Here $\mu = \cos(\theta)$, and the angles $\theta$, $\theta_1$, and $\theta_2$ are defined as $\theta = \hat{r}_a \Lambda \hat{r}_b$ and $\theta_i = \hat{r}_b \Lambda \hat{r}_i$ ($i = 1$ and $2$). See Ref. 10 for other notation.

The use of the form (9), rather than that of Austern et al.[11,12] not only helps to make the following argument much more transparent, but also has been vital in making the calculations of Refs. 2-5 possible. As emphasized in Ref. 10, the Austern form becomes very inconvenient to use if $l$ exceeds a certain value which is rather small, say 5, because a very difficult problem of truncation error emerges. With the form of (9), we do not encounter this numerical problem, and so this form is in fact used in the step of evaluating the EFR-DWBA overlap integrals, from which our parametrization procedure starts. Since we are concerned with transitions to the continuum, we encounter very large $l$ values, which may easily go beyond 20.

Returning to the main subject of the present section, we first note that the integrand of the integral over $\mu$, appearing in (9), is peaked very sharply in the extreme neighborhood of $\mu = 1$. In the present example of the $(^{14}N, {}^{12}B)$ reaction, it is not difficult to show that the range of $\mu$ over which the above integration must be carried out is given by $\mu = 0.9995 \sim 1$. The reason why such an extremely narrow range of integration is encountered is the same as is given for a similar integral that appeared in the Austern form of the form factor, explained in detail in Ref. 12.

The fact that $\mu$ remains very close to unity results in another localization: that the integral in (9) can have significant values only when $|m_l|$ is very small, $|m_l| = 0$, and possibly $= 1$. This is because $l_a$ is normally large, and thus $|Y_{l_a m_l, 1}(\mu)| \ll |Y_{l_a m_l}(\mu)|$, if $\mu \approx 1$. Thus the summation over $m_l$ is very limited. The summation over $m_2$ is also limited because $|m_2| \le l_2 = 2$. Because of the second Clebsch-Gordan (CG) coefficient in (9), which requires that $m_1 + m_2 = m_l$, the allowed range of $m_1$ is also narrow. We may remark further that the factor $Y_{l_1 m_1}(\theta_1)$ in the integrand in (9) also has a tendency to make the integral smaller as $|m_1|$ gets larger.

Having in mind the restriction of $|m_l|$ to 0 and 1, we may now remark that the $m_l = 0$ term in (9) gives the no-recoil part of the form factor, while that with $m_l = 1$ contributes the recoil correction. Note that we mean by "recoil" only the so-called *transverse* part of recoil. The *longitudinal* recoil is included in both the $|m_l| = 0$ and 1 terms.

We shall now rewrite the expression of (9) somewhat, by taking particular advantage of the severely restricted sum over the magnetic quantum numbers. For simplicity, we shall henceforth denote the integral factor in (9) simply by $i(m_l, m_1, m_2)$, and then introduce further the ratios $P_0 = i(0, 1, -1)/i(0, 0, 0)$, $P_1 = i(1, 0, -1)/i(0, 0, 0)$, $P_2 = i(1, -1, 0)/i(0, 0, 0)$, and $P_3 = i(1, 1, -2)/i(0, 0, 0)$. It is then a straightforward matter to find that (9) can be replaced by

$$F_{l_b l_a}^{l_1 l_2}(r_b, r_a) = \tfrac{1}{2}[(4\pi)^{3/2}/(2l+1)]\hat{l}_b i^{l_a + l_b + l} 1^{+l} l_2 (-)^l i(0,0,0)$$
$$\times \{(l_a 0 l_b 0 | l0)[(l_1 0 l_2 0 | l0) + 2(l_1 l_2 - 1 | l0)P_0]$$
$$- 2(l_a 1 l_b 0 | l1)[(l_1 0 l_2 - 1 | l-1)P_1 - (l_1 - 1 l_2 0 | l-1)P_2 + (l_1 1 l_2 - 2 | l-1)P_3]\}. \tag{10}$$

It is clear that the terms involving $P_1$, $P_2$, and $P_3$ factors are the recoil terms. We also remark here that the ratios $P_0 \sim P_3$ are all positive. Keep in mind that they are the ratios of the integrals of (9) taken at the values of $r_a$ and $r_b$ where the form factors take their maximum values.

The expression of (10) can be brought further into a much more transparent form. To do this, we first mention the approximate relations

$$(l_a 1 l_b 0 | l1) \simeq \begin{cases} -(l_d/2l)(l_a 0 l_b 0 | l0) & (l_a + l_b + l = \text{even}), \\ [1 - (l_d/l)^2]^{1/2}(l_a 0 l_b 0 | l + 1 0) \end{cases}$$

$$(l_a + l_b + l = \text{odd}), \tag{11}$$

which are derived by using recursion relations between CG coefficients.[13] We may also note the relation

$$(l_a 0 l_b 0 | l0) \simeq (4e/\pi)^{1/2} \hat{l}_b^{-1}[1 + (l_d/2l)^2] i^{l_a + l_b - l}, \tag{12}$$

which is obtained by using Stirling's formula to evaluate the factorials in terms of which the parity-conserving CG coefficients are expressed.

Using (11) and (12), and the explicit forms of the CG coefficients involving $l_2 = 2$, we can now rewrite (10) as

$$F_{l_b l_a}^{l_1 l_2}(r_b, r_a) \simeq \tfrac{1}{2}[(4\pi)^{3/2}/(2l+1)][(4e/\pi)]^{1/2}$$
$$\times i(0,0,0)[1 + (l_d/2l)^2]\chi_\Delta, \tag{13a}$$

where

$$\chi_\Delta = \begin{cases} \tfrac{3}{8}[1 \pm \tfrac{8}{3}P_0 - (l_d/l)(P_1 \pm \tfrac{2}{3}P_2)] & (\Delta = \pm 2), \\ \tfrac{1}{2}[1 - \tfrac{1}{2}(l_d/l)^2](P_2 \pm P_3) & (\Delta = \pm 1), \\ \tfrac{1}{2}[1 - (l_d/l)P_1] & (\Delta = 0). \end{cases} \tag{13b}$$

This is the final expression of the form factor we wanted to derive. We shall now show that this expression does contain in it every feature which the curves given in Fig. 3(b) reveal in themselves.

For simplicity of presentation, let us denote by $F(\Delta)$ the five expressions on the right-hand side of (13). As we noted above, all the $P$'s are positive. We further note here that $P_0$, $P_1$, and $P_2$ are of the same order of magnitude, being close but somewhat smaller than unity, while $P_3$ is much smaller. From these properties of the $P$'s, one may easily deduce the following properties of the $F(\Delta)$.

(i) At $l_d = 0$, an inequality $F(2) > F(0) > F(-2)$ $> F(1) > F(-1)$ should hold. (ii) For all $l_d$, an inequality $F(1) > F(-1)$ should hold, although the difference between $F(1)$ and $F(-1)$ is small (since $P_3$ $< P_2$). (iii) For all $l_d$, $F(1)$ and $F(-1)$ should both depend on $l_d$ like $[1 - \frac{1}{4}(l_d/l)^2]$. (iv) For all $l_d$, $F(2)$ should depend on $l_d$ as does $[1 + (l_d/l)^2]$, if (and in fact since) $P_1 - \frac{2}{3}P_2 \approx 0$. (v) $F(-2)$ and $F(0)$ should decrease almost linearly, as $l_d$ increases, the former having a slope steeper than that in the latter. [This is seen from the last terms of $F(-2)$ and $F(0)$, and the fact that $P_1 + \frac{2}{3}P_2 > P_1$.] (vi) The $l_d$ dependence discussed in the last three of the above items should get weaker as $l_1$ is increased. [This is because $l_d$ appears in (13) always in the form of $l_d/l$, and because $l = l_1 + \Delta$.]

All the expectations enumerated in the above items (i)–(vi) are seen to be fulfilled by the curves given in Fig. 3(b), at least qualitatively, and in many cases even quantitatively, with possibly only one exception, namely that (ii) is violated slightly when $l_1 = 6$ and $l_d < 0$. We may thus say that we now have a nearly perfect understanding of the behavior of (the peak values of) the form factor. We may emphasize here that the complicated $\Delta$ dependence of $F(\Delta)$ is almost entirely due to the recoil effect, and we have now succeeded in understanding very clearly this $\Delta$ dependence of the recoil effect.

In the item (vi) above, we referred very briefly to the $l_1$ dependence of the form factor. There remains, however, one more very important $l_1$ dependence to be pointed out and to be explained. It is that the overall magnitude of the form factor decreases as $l_1$ is increased, which can be seen by comparing the two sets of curves in Fig. 3b, one for $l_1 = 6$ and the other for $l_1 = 10$. This $l_1$ dependence of the form factor can be traced back to that of the factor $i(0,0,0)$ in (13), and is explained as follows.

The factor $i(0,0,0)$ is nothing but the integral in (9), when all the magnetic quantum numbers there are set equal to zero. The factor $Y_{l_d 0}(\mu)$ in the integrand has its maximum value at $\mu = 1$, and de-

creases very rapidly as $\mu$ deviates from 1. Since $\cos\theta_1 = 1$, when $\mu = 1$, (see Ref. 10) the factor $Y_{l_1 0}(\theta_1)$ is also peaked at $\mu = 1$, and decreases as $\mu$ is decreased. When $l_1$ is small, however, $Y_{l_1 0}(\theta_1)$ remains essentially unchanged within the very narrow range of the $\mu$ integral, which we discussed above. However, if $l_1$ is large, the deviation of $Y_{l_1 0}(\theta_1)$ from its peak value becomes non-negligible, making the integrand smaller than it is otherwise. This is the reason why $i(0,0,0)$ decreases as $l_1$ increases. In this way the last remaining $l_1$ dependence of the form factor is understood.

Since the behavior of the form factor has now been well understood, so is that of the factor $N_0$. After all, the similarity of the behaviors of the form factor and of $N_0$ are also easy to understand. As can be seen from (2a), $N_0$ is nothing but the magnitude of the overlap integral itself, when the latter is obtained under the restriction that both $l_b$ and $l_d$ have their respective window values, i.e., that the best conceivable kinematic matching is established. The overlap integrals that are selected under such severe restrictions will have to depend on nothing other than the peak values of the underlying form factors.

## IV. FINAL REMARKS

We have shown that the EFR-DWBA overlap integrals can be represented rather well by a fairly simple analytic function, with a few parameters in it. Once this parametrization is carried out, the calculation of the DWBA cross section can be done in a well known way; it is the same irrespective of whether the overlap integrals are given in a parametrized form or not. This cross section, which we may simply denote as $\sigma_{DW}$, is a function of $Q$, $I_B$ $(=l_1)$ and $l$. In order to use this $\sigma_{DW}$ to obtain the continuum cross section $\sigma$, it must further be combined with another function which we call[1-5] the spectroscopic density and denote by $\rho_s$. This function $\rho_s$ depends on $I_B$, as well as on $E_x$, the excitation energy of the residual nucleus, which is given by $E_x = Q_{gr} - Q$, where $Q_{gr}$ is the $Q$ value corresponding to the ground-state-to-ground-state transition. More explicitly we may get

$$\sigma(Q, \theta) = \sum_{I_B} \left\{ \sum_l \sigma_{DW}(I_B, Q, l, \theta) \right\} \rho_s(E_x, I_B). \quad (14)$$

As is clear from (14), the explanation of how to use the direct reaction theory to fit the continuum cross sections remains incomplete, until the way to construct $\rho_s$ is explained. This has been done, however, in our previous publications, though it was somewhat cursory.[1-5] We shall not repeat it here, but intend to rediscuss it in a somewhat

more systematic way in a forthcoming paper,[14] in which the calculations made in Refs. 2–5 will be reviewed in detail.

As we emphasized above, the behavior of the factor $N_0$ was fairly complicated, largely because we chose, as an example, the case which has $l_2 = 2$. In the very simple case with $l_2 = 0$, the peak values of the form factor are simply given by (13) retaining only the term with $\Delta = 0$, after replacing $P_1$ there by $P_2$. Thus the reader will find it very easy to apply our method, if his interest is limited to the case with $l_2 = 0$.

We finally want to remark that our discussions given in the present paper have been limited to the use of the *one-step* DWBA theory. We have seen in Refs. 2–5 that a variety of data could be explained, even if this restriction was made. We also saw, however, in these same works, that (part of) the data indicated the necessity of con-

sidering higher-order contributions as well. In Ref. 2, an example was given of how to use the parametrized form of the one-step DWBA overlap integrals, in order to obtain the amplitudes of the two-step processes. Although it was found[2] that this method worked rather well also, it was also clear that the calculations involved were rather tedious. It is thus very desirable to find a method to parametrize the two- (and possibly still higher-) step amplitudes in a much more direct way. An investigation of such a possibility is under way.

[1]T. Tamura, T. Udagawa, D. H. Feng, and K. K. Kan, Phys. Lett. 66B, 109 (1977). T. Tamura and T. Udagawa, *ibid.* 71B, 273 (1977); 78B, 189 (1978).

[2]T. Udagawa, T. Tamura, and B. T. Kim, Phys. Lett. 82B, 349 (1978).

[3]T. Udagawa and T. Tamura, Phys. Rev. Lett. 41, 1770 (1978); 42, 1501 (1979).

[4]H. Frolich, T. Shimoda, M. Ishihara, K. Nagatani, T. Udagawa, and T. Tamura, Phys. Rev. Lett. 42, 1518 (1979).

[5]M. Ishihara, T. Shimoda, H. Frolich, H. Kamitsubo, K. Nagatani, T. Udagawa, and T. Tamura, Phys. Rev. Lett. 43, 111 (1979).

[6]V. Strutinsky, Zh. Eksp. Teor. Fiz. 46, 2078 (1964) [Soviet Phys.—JETP 19, 1401 (1964)].

[7]S. Kahana and A. J. Baltz, *Advances in Nuclear Physics,* edited by M. Baranger and E. Vogt (Plenum, New York, 1977), Vol. 9, p. 1.

[8]J. B. Natowitz, N. M. Namboodiri, I. Eggers, P. Gonthier, K. Goeffroy, R. Hanus, C. Towsley, and K. Das, Nucl. Phys. A277, 477 (1977).

[9]K. Sugimoto, N. Takahashi, A. Mizobuchi, Y. Nojiri, T. Minamisono, M. Ishihara, K. Tanaka, and H. Kamitsubo, Phys. Rev. Lett. 39, 323 (1977).

[10]T. Tamura, T. Udagawa, and H. Amakawa, Prog. Theor. Phys. 60, 1238 (1978). T. Tamura, T. Udagawa, K. E. Wood, and H. Amakawa, Comp. Phys. Commun. 18, 163 (1979).

[11]N. Austern, R. M. Drisco, E. C. Halbert, and G. R. Satchler, Phys. Rev. 133, B3 (1964).

[12]T. Tamura, Phys. Rep. 14C, 59 (1974).

[13]D. M. Brink and G. R. Satchler, *Angular momentum* (Oxford University Press, London, 1968).

[14]T. Udagawa, T. Tamura, and K. Nagatani (unpublished).